Comparison of Adaptive and Conventional Backstepping Super-Twisting Sliding Mode Controls for Trajectory Tracking of an Autonomous Underwater Vehicle

Warit Tanaprasitpattana[1], Peerayot Sanposh[1]*, Benjaset Maneeloke[1], Nattakit Techajaroonjit[2], Vasutorn Siriyakorn[1], Yodyium Tipsuwan[2] and Weerawut Charubhun[3]

[1]Department of Electrical Engineering, Faculty of Engineering, Kasetsart University
[2]Department of Computer Engineering, Faculty of Engineering, Kasetsart University
[3]Rovula, AI and Robotics Ventures Company Limited, PTTEP, Bangkok, Thailand

Abstract: Maritime missions involving autonomous underwater vehicles (AUVs) often encounter uncertainties and external disturbances, posing significant challenges for trajectory tracking. These challenges complicate the design of controllers capable of achieving high-precision trajectory tracking. This paper proposes a comparison between the backstepping super-twisting sliding mode control (BSTSMC) and the novel adaptive backstepping super-twisting sliding mode control (ABSTSMC) approach for trajectory tracking of AUVs in 6 degrees of freedom (DOF) under thruster fault conditions. The ABSTSMC method retains the benefits of robust control while incorporating adaptive techniques to minimize the impact of unknown external disturbances and thruster faults by adjusting the gain online. The performance of both BSTSMC and ABSTSMC is evaluated and compared through simulation results using ROS2, with a focus on their ability to handle external disturbances and thruster faults.

***Keywords*— Autonomous Underwater Vehicle (AUV), Adaptive Backstepping Control (ABC), Super-Twisting Sliding Mode Control (STSMC), Thruster Fault**

I. Introduction

Autonomous underwater vehicles (AUVs) are increasingly employed in various underwater missions such as oceanographic surveys, environmental monitoring, military operations, submarine oil pipeline detection, and underwater rescue. These missions often require precise trajectory tracking capabilities in challenging underwater environments characterized by uncertainties and disturbances.

In recent years, various control techniques have been developed to enhance the trajectory tracking performance of AUVs. The efficiency of these controllers is heavily based on various factors, particularly the underlying mathematical model. A prominent example is an influential mathematical model of AUV proposed by Fossen, as outlines in [1-2]. This model also integrates environmental forces, such as ocean currents, into motion equations, significantly impacting AUV control. Designing a controller for high tracking accuracy is challenging because of the uncertain parameters in the AUV model, nonlinearity, and unknown external disturbance. In recent years, various controllers have been developed to solve many trajectory tracking issues for AUVs.

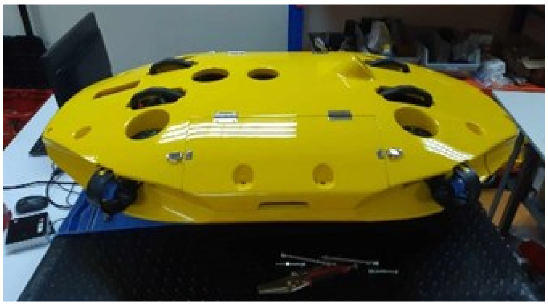

Fig. 1. The Xplorer-mini AUV, equipped with eight thrusters, developed at Autonomous Marine Research Lab (AMARR Lab) at Faculty of Engineering, Kasetsart University

Conventional control methods, such as Proportional-Derivative (PD) and Proportional-Integral-Derivative (PID) controllers, are commonly applied because of their straightforward implementation. However, PD controllers require accurate knowledge of buoyancy and gravitational force [1], while PID controllers face performance issues in nonlinear, time-varying system [3]. To overcome these challenges, advanced control techniques have been developed to address uncertainties and disturbances effectively.

Adaptive control approaches have been widely investigated to improve AUV performance in uncertain conditions. For instance [4] introduced terminal sliding mode control for underactuated AUVs, demonstrating accurate trajectory tracking. Similarly [5] presented a modified C/GMRES-based predictive controller for efficient nonlinear tracking. In certain studies, the

The manuscript received Sept. 10, 2024; revised Dec. 24, 2024; accepted Dec. 28, 2024; Date of publication Dec. 30, 2024

*Corresponding author: Peerayot Sanposh, Department of Electrical Engineering, Faculty of Engineering, Kasetsart University, Bangkok 10900, Thailand (E-mail: fengpyp@ku.ac.th)

integration of adaptive control with intelligent control has been suggested, including approaches like Neural Network-based Control (NNC) [6], [7], Fuzzy Logic Controllers (FTC) [8] and Reinforcement Learning (RL) [9], [10].

Sliding Mode Control (SMC) is recognized for its robustness in handling external disturbances and system uncertainties. High-Order Sliding Mode Control (HOSMC) [18] techniques further address the chattering issue observed in conventional SMC methods, providing smoother control signals [11], [12]. For example [13] proposed a robust adaptive sliding mode controller to manage uncertain dynamics effectively. The controller is designed using dual closed-loop control approach, where the outer loop determines virtual velocity commands, and the inner loop generates the actual control inputs. However, the paper notes that the stability analysis for the outer-loop and inner-loop systems is performed independently, potentially neglecting the interactions between the loops. This could result in suboptimal performance in practical applications. It further states that all tracking errors in the closed-loop systems are uniformly ultimately bounded, as demonstrated through Lyapunov stability analysis. This indicates that while the errors may not converge to zero in finite time, they will remain within a certain boundary over time.

Backstepping-based sliding mode control has shown promise for stabilizing complex nonlinear systems, particularly under external disturbances [14]. Recent advancements in adaptive control have led to improved accuracy in trajectory tracking. For example, Peng et al. [15] proposed a dual closed-loop MPC strategy to handle uncertainties which is the combination of backstepping and optimal control, while [16] developed an adaptive backstepping sliding mode controller for lightweight AUVs with input saturation. However, both studies assume that external disturbance is bound and predictable. This assumption may limit the approach's effectiveness in handling unbounded external perturbations, potentially impacting real-world implementation.

Although these methods have demonstrated success, comprehensive comparisons of their performance under practical conditions remain limited. Notably, integrating super-twisting algorithms into backstepping controllers has shown significant improvements in robustness and chattering reduction [17]. However, the effectiveness of adaptive versus conventional backstepping super-twisting sliding mode controllers has yet to be fully explored.

This paper presents two advanced control strategies for trajectory tracking of the 6-DOF Xplorer-mini AUV, equipped with eight thrusters and developed at the Autonomous Marine Research Lab (AMARR Lab) at Faculty of Engineering, Kasetsart University, as shown in Fig. 1. The proposed strategies are the Backstepping Super-Twisting Sliding Mode Control (BSTSMC) and the Adaptive Backstepping Super-Twisting Sliding Mode Control (ABSTSMC). The ABSTSMC enhances the robustness of the BSTSMC by incorporating adaptive backstepping to address system nonlinearities and uncertainties, particularly under thruster faults. The key contributions of this study are:

1. A detailed comparative analysis of the two approaches in terms of tracking accuracy, disturbance rejection, and robustness, especially under a thruster fault.
2. Stability analysis via Lyapunov function.

The structure of this paper is as follows: Section II presents the mathematical modeling of the AUV. Section III provides the design details of the proposed BSTSMC and ABSTSMC approach. Section IV discusses the simulation results, and Section V concludes the paper with final remarks and our future research work.

II. Modeling

The mathematical model of an AUV is described in two coordinate frames: the body-fixed frame and earth-fixed frame. The kinematic and dynamic equations of an AUV in 6-DOF can be written as follows [1]:

$$\begin{gathered} \dot{\boldsymbol{\eta}} = \boldsymbol{J}(\boldsymbol{\eta})\boldsymbol{\nu} \\ \boldsymbol{M}_{RB}\dot{\boldsymbol{\nu}} + \boldsymbol{M}_A\dot{\boldsymbol{\nu}}_r + \boldsymbol{C}_{RB}(\boldsymbol{\nu})\boldsymbol{\nu} + \boldsymbol{C}_A(\boldsymbol{\nu}_r)\boldsymbol{\nu}_r + \boldsymbol{D}(\boldsymbol{\nu}_r)\boldsymbol{\nu}_r \\ + \boldsymbol{g}(\boldsymbol{\eta}) = \boldsymbol{\tau} + \boldsymbol{\tau}_{dist} \end{gathered} \tag{1}$$

where $\boldsymbol{\nu} = [u, v, w, p, q, r]^T$ is the AUV linear and angular velocity vector relative to the body-fixed frame, $\boldsymbol{\eta} = [x, y, z, \phi, \theta, \psi]^T$ is the AUV position and orientation vector relative to the earth-fixed frame, $\boldsymbol{\nu}_r = \boldsymbol{\nu} - \boldsymbol{\nu}_c$ is the relative velocity of the AUV, $\boldsymbol{\nu}_c$ is the irrotational ocean current velocity relative to the body-fixed frame, $\boldsymbol{M}_{RB}$ is the rigid-body inertia matrix, $\boldsymbol{M}_A$ is the added mass matrix from hydrodynamic effects, $\boldsymbol{C}_{RB}(\boldsymbol{\nu})$ is the rigid-body Coriolis and centripetal matrix, $\boldsymbol{C}_A(\boldsymbol{\nu}_r)$ is the hydrodynamic Coriolis and centripetal matrix, $\boldsymbol{D}(\boldsymbol{\nu}_r)$ is the hydrodynamic damping matrix, $\boldsymbol{g}(\boldsymbol{\eta})$ is the restoring force and moment vector from the gravitational and buoyancy forces, $\boldsymbol{\tau}$ is the control force and moment vector generated by thrusters, $\boldsymbol{\tau}_{dist}$ is the disturbance force and moment vector, and $\boldsymbol{J}(\boldsymbol{\eta})$ is the transformation matrix given by:

$$\boldsymbol{J}(\boldsymbol{\eta}) = \begin{bmatrix} \boldsymbol{R}_b^n(\boldsymbol{\Theta}_{nb}) & 0 \\ 0 & \boldsymbol{T}(\boldsymbol{\Theta}_{nb}) \end{bmatrix} \tag{2}$$

where $\boldsymbol{\Theta}_{nb} = [\phi, \theta, \psi]^T$ is the AUV orientation described by the Euler angles, $\boldsymbol{R}_b^n(\boldsymbol{\Theta}_{nb})$ is the rotation matrix, and $\boldsymbol{T}(\boldsymbol{\Theta}_{nb})$ is the transformation matrix.

The tracking problem is posted by giving $\boldsymbol{\eta}_d(t)$, the AUV state vector is selected as $[\boldsymbol{\eta}, \dot{\boldsymbol{\eta}}]^T$. After the kinematic transformation process, the dynamic equation (1) can be written as:

$$\begin{aligned} &\boldsymbol{M}_\eta\ddot{\boldsymbol{\eta}} + \boldsymbol{C}_\eta\dot{\boldsymbol{\eta}} + \boldsymbol{D}_\eta\dot{\boldsymbol{\eta}} + \boldsymbol{g}_\eta \\ &\quad = \boldsymbol{\tau} + \boldsymbol{\tau}_{dist} + \boldsymbol{M}_A\dot{\boldsymbol{\nu}}_c + \boldsymbol{C}_A(\boldsymbol{\nu}_r)\boldsymbol{\nu}_c \\ &\quad + \boldsymbol{D}(\boldsymbol{\nu}_r)\boldsymbol{\nu}_c \end{aligned} \tag{3}$$

where

$$\begin{aligned} \boldsymbol{M}_\eta &= (\boldsymbol{M}_{RB} + \boldsymbol{M}_A)\boldsymbol{J}^{-1}(\boldsymbol{\eta}) \\ \boldsymbol{C}_\eta &= [\boldsymbol{C}_{RB}(\boldsymbol{\nu}) + \boldsymbol{C}_A(\boldsymbol{\nu}_r)]\boldsymbol{J}^{-1}(\boldsymbol{\eta}) - \boldsymbol{M}_\eta\dot{\boldsymbol{J}}(\boldsymbol{\eta})\boldsymbol{J}^{-1}(\boldsymbol{\eta}) \\ \boldsymbol{D}_\eta &= \boldsymbol{D}(\boldsymbol{\nu}_r)\boldsymbol{J}^{-1}(\boldsymbol{\eta}) \\ \boldsymbol{g}_\eta &= \boldsymbol{g}(\boldsymbol{\eta}) \end{aligned}$$

III. Methodology

In this section, we present two control methods combining backstepping with the Super-Twisting Algorithm (STA), a higher order sliding mode control introduced in [19]. The design of an adaptive control law based on the original Super-Twisting (STW) control is presented in [20] and further summarized in [21], [22]. Let

$\boldsymbol{u} = \boldsymbol{\tau}$ be the desired control force and moment vector from AUV controller. The proposed control $\boldsymbol{u}$ can be written as:

$$\boldsymbol{u} = \boldsymbol{u}_{nc} + \boldsymbol{u}_{sc} \tag{4}$$

where $\boldsymbol{u}_{nc}$ is the nominal control, and $\boldsymbol{u}_{sc}$ is the switching control that is used to handle disturbances and thruster faults.

A. BSTSMC: Backstepping Super-Twisting Sliding Mode Control

Let $\boldsymbol{x}_1 = \boldsymbol{\eta}$ and $\boldsymbol{x}_2 = \dot{\boldsymbol{\eta}}$ is the AUV state vector. From (3), the AUV state-space model can be written as:

$$\dot{\boldsymbol{x}} = \begin{bmatrix}\dot{\boldsymbol{x}}_1\\ \dot{\boldsymbol{x}}_2\end{bmatrix} = \begin{bmatrix}\boldsymbol{x}_2\\ \boldsymbol{a}(\boldsymbol{x}) + \boldsymbol{b}(\boldsymbol{x})\boldsymbol{u} + \boldsymbol{d}\end{bmatrix} \tag{5}$$

where

$$\begin{aligned}\boldsymbol{a}(\boldsymbol{x}) &= (\boldsymbol{M}_\eta)^{-1}[-\boldsymbol{C}_\eta\dot{\boldsymbol{\eta}} - \boldsymbol{D}_\eta\dot{\boldsymbol{\eta}} - \boldsymbol{g}_\eta + \boldsymbol{C}_A(\boldsymbol{v}_r)\boldsymbol{v}_c \\ &\quad + \boldsymbol{D}(\boldsymbol{v}_r)\boldsymbol{v}_c] \\ \boldsymbol{b}(\boldsymbol{x}) &= (\boldsymbol{M}_\eta)^{-1} \\ \boldsymbol{d} &= (\boldsymbol{M}_\eta)^{-1}[\boldsymbol{M}_A\dot{\boldsymbol{v}}_c - \boldsymbol{\tau}_{dist}]\end{aligned}$$

Define the position/orientation tracking error as:

$$\boldsymbol{z}_1 = \boldsymbol{x}_1 - \boldsymbol{\eta}_d \tag{6}$$

Then, using the backstepping method, the virtual velocity control $\boldsymbol{\alpha}_{virtual}$ is chosen as:

$$\boldsymbol{\alpha}_{virtual} = -\boldsymbol{K}_1\boldsymbol{z}_1 + \dot{\boldsymbol{\eta}}_d \tag{7}$$

where $\boldsymbol{K}_1 \in \mathbb{R}^{6\times6}$ is symmetric positive definite. Next, the virtual velocity tracking error $\boldsymbol{z}_2$ is defined as:

$$\boldsymbol{z}_2 = \boldsymbol{x}_2 - \boldsymbol{\alpha}_{virtual} \tag{8}$$

From (5), (6), (7), and (8), the dynamic equation of $\boldsymbol{z} = [\boldsymbol{z}_1, \boldsymbol{z}_2]^T$ can be written as:

$$\dot{\boldsymbol{z}} = \begin{bmatrix}\dot{\boldsymbol{z}}_1\\ \dot{\boldsymbol{z}}_2\end{bmatrix} = \begin{bmatrix}-\boldsymbol{K}_1\boldsymbol{z}_1 + \boldsymbol{z}_2\\ \boldsymbol{a}(\boldsymbol{x}) + \boldsymbol{b}(\boldsymbol{x})\boldsymbol{u} + \boldsymbol{d} - \dot{\boldsymbol{\alpha}}_{virtual}\end{bmatrix} \tag{9}$$

Consider the sliding variable:

$$\boldsymbol{\sigma} = \boldsymbol{K}_2\boldsymbol{z}_1 + \boldsymbol{z}_2 \tag{10}$$

where $\boldsymbol{K}_2 \in \mathbb{R}^{6\times6}$ is a diagonal matrix, whose elements are positive. The time derivative of the sliding variable is given by:

$$\dot{\boldsymbol{\sigma}} = \boldsymbol{K}_2\dot{\boldsymbol{z}}_1 + \dot{\boldsymbol{z}}_2 \tag{11}$$

The Lyapunov candidate function is chosen as:

$$V = \frac{1}{2}\boldsymbol{z}_1^T\boldsymbol{z}_1 + \frac{1}{2}\boldsymbol{\sigma}^T\boldsymbol{\sigma} \tag{12}$$

Then, the time derivative of is given by:

$$\dot{V} = \boldsymbol{z}_1^T\dot{\boldsymbol{z}}_1 + \boldsymbol{\sigma}^T\dot{\boldsymbol{\sigma}} \tag{13}$$

From (9) and (11), (13) can be rearranged as:

$$\begin{aligned}\dot{V} &= \boldsymbol{z}_1^T(-\boldsymbol{K}_1\boldsymbol{z}_1 + \boldsymbol{z}_2) \\ &\quad + \boldsymbol{\sigma}^T(\boldsymbol{K}_2\dot{\boldsymbol{z}}_1 + \boldsymbol{a}(\boldsymbol{x}) + \boldsymbol{b}(\boldsymbol{x})\boldsymbol{u} \\ &\quad + \boldsymbol{d} - \dot{\boldsymbol{\alpha}}_{\text{virtual}})\end{aligned} \tag{14}$$

From (4) and (14), $\boldsymbol{u}_{nc}$ is given by:

$$\begin{aligned}\boldsymbol{u}_{nc} &= (\boldsymbol{b}(\boldsymbol{x}))^{-1}[-\boldsymbol{K}_3\boldsymbol{\sigma} - \boldsymbol{K}_2^{-1}\boldsymbol{z}_2 - \boldsymbol{K}_2\dot{\boldsymbol{z}}_1 - \boldsymbol{a}(\boldsymbol{x}) \\ &\quad + \dot{\boldsymbol{\alpha}}_{virtual}]\end{aligned} \tag{15}$$

where $\boldsymbol{K}_3 \in \mathbb{R}^{6\times6}$ is diagonal matrix with positive elements. The switching control $\boldsymbol{u}_{sc}$ is designed as:

$$\begin{aligned}\boldsymbol{u}_{sc} &= (\boldsymbol{b}(\boldsymbol{x}))^{-1}[-\boldsymbol{\alpha}|\boldsymbol{\sigma}|^{1/2}\text{sign}(\boldsymbol{\sigma}) + \boldsymbol{v}] \\ \dot{\boldsymbol{v}} &= -\boldsymbol{\beta}\text{sign}(\boldsymbol{\sigma})\end{aligned} \tag{16}$$

where $|\boldsymbol{\sigma}|^{1/2}\text{sign}(\boldsymbol{\sigma}) = [|\sigma_1|^{1/2}\text{sign}(\sigma_1), \dots, |\sigma_6|^{1/2}\text{sign}(\sigma_6)]^T$ and $\text{sign}(\boldsymbol{\sigma}) = [sgn(\sigma_1), \dots, sgn(\sigma_6)]^T$.

From (15) and (16), (14) can be rearranged as:

$$\begin{aligned}\dot{V} &= -\boldsymbol{z}_1^T\boldsymbol{K}_1\boldsymbol{z}_1 - \boldsymbol{z}_2^T\boldsymbol{K}_2^{-1}\boldsymbol{z}_2 - \boldsymbol{\sigma}^T\boldsymbol{K}_3\boldsymbol{\sigma} \\ &\quad - \boldsymbol{\sigma}^T\left[\boldsymbol{\alpha}|\boldsymbol{\sigma}|^{\frac{1}{2}}\text{sign}(\boldsymbol{\sigma}) + \int_0^t \boldsymbol{\beta}\text{sign}(\boldsymbol{\sigma}(\tau))d\tau - d\right] \\ \dot{V} &= -\boldsymbol{z}_1^T\boldsymbol{K}_1\boldsymbol{z}_1 - \boldsymbol{z}_2^T\boldsymbol{K}_2^{-1}\boldsymbol{z}_2 - \boldsymbol{\sigma}^T\boldsymbol{K}_3\boldsymbol{\sigma} \\ &\quad - \sum_{i=1}^{6}\left[\alpha_i|\sigma_i|^{1/2}|\sigma_i| + \beta_i\sigma_i\int_0^t \text{sign}(\sigma_i(\tau))d\tau - d_i\sigma_i\right]\end{aligned}$$

where $\boldsymbol{\alpha} = \text{diag}(\alpha_1, \alpha_2, \dots, \alpha_6)$, $\alpha_i > 0$ and $\boldsymbol{\beta} = \text{diag}(\beta_1, \beta_2, \dots, \beta_6)$, $\beta_i > 0$.

Under the assumption that $|d_i| \le \delta_i|\sigma_i|^{1/2}$ for some unknown $\delta_i > 0$, and by selecting $\alpha_i > \delta_i$, we have:

$$d_i\sigma_i \le |d_i\sigma_i| \le \delta_i|\sigma_i|^{1/2}|\sigma_i| < \alpha_i|\sigma_i|^{1/2}|\sigma_i|$$

With appropriate tuning of α_i and β_i, and under finite-time operation condition, we can conclude that:

$$\sum_{i=1}^{6}\left[\alpha_i|\sigma_i|^{1/2}|\sigma_i| + \beta_i\sigma_i\int_0^t \text{sign}(\sigma_i(\tau))d\tau - d_i\sigma_i\right] > 0$$

Consequently, $\dot{V}$ is negative- definite. By Barbalat' s Lemma, the tracking error converges asymptotically to zero.

B. ABSTSMC: Adaptive Backstepping Super-Twisting Sliding Mode Control

For the ABSTSMC, the adaptive law is given by:

$$\begin{aligned}\dot{\alpha}_i &= \begin{cases}\omega_{1i}\sqrt{\dfrac{\gamma_{1i}}{2}}, & \text{if } \boldsymbol{\sigma} \ne 0\\ 0, & \text{if } \boldsymbol{\sigma} = 0\end{cases} \\ \beta_i &= 2\varepsilon_i\alpha_i + \lambda_i + 4\varepsilon_i^2\end{aligned} \tag{17}$$

where $\omega_{1i}, \gamma_{1i}, \varepsilon_i$ and λ_i are arbitrary positive constants. This ABSTSMC makes $\boldsymbol{\sigma}$ and $\dot{\boldsymbol{\sigma}}$ go to zero in finite time [19].

Now, the finite-time convergence of $\boldsymbol{\sigma}$ and $\dot{\boldsymbol{\sigma}}$ is proved. We rearrange (11) using (9), (15) and (16) as follows:

$$\dot{\boldsymbol{\sigma}} = (-\boldsymbol{K}_3\boldsymbol{\sigma} - \boldsymbol{K}_2^{-1}\boldsymbol{z}_2 + \boldsymbol{d}) + \boldsymbol{b}(\boldsymbol{x})\boldsymbol{u}_{sc}$$

which can be expressed as:

$$\dot{\boldsymbol{\sigma}} = \boldsymbol{\Psi}(\boldsymbol{z}, \boldsymbol{d}, t) + \boldsymbol{\Gamma}(\boldsymbol{z}, t)\boldsymbol{u}_{sw} \tag{18}$$

where $\boldsymbol{\Psi}(\boldsymbol{z}, \boldsymbol{d}, t) = -\boldsymbol{K}_3\boldsymbol{\sigma} - \boldsymbol{K}_2^{-1}\boldsymbol{z}_2 + \boldsymbol{d}$, $\boldsymbol{\Gamma}(\boldsymbol{z}, t) = \mathbf{I}_{6\times6}$ and $\boldsymbol{u}_{sw} = \boldsymbol{b}(\boldsymbol{x})\boldsymbol{u}_{sc}$.

From (16), we further rearrange (18) into the form:

$$\begin{aligned}\dot{\boldsymbol{\sigma}} &= -\boldsymbol{\alpha}|\boldsymbol{\sigma}|^{1/2}\text{sign}(\boldsymbol{\sigma}) + \boldsymbol{v} + \boldsymbol{\Psi}(\boldsymbol{z}, \boldsymbol{d}, t) \\ \dot{\boldsymbol{v}} &= -\boldsymbol{\beta}\text{sign}(\boldsymbol{\sigma})\end{aligned} \tag{19}$$

Then, (19) can be rewritten in scalar form as:

$$\begin{aligned}\dot{\sigma}_i &= -\alpha_i|\sigma_i|^{1/2}\text{sign}(\sigma_i) + v_i + \Psi_i(\boldsymbol{z}, \boldsymbol{d}, t)\\ \dot{v}_i &= -\beta_i\text{sign}(\sigma_i)\end{aligned} \quad (20)$$

Consider the following Lyapunov candidate function [19]:

$$V_2 = \sum_{i=1}^{6} V_{2i} = \sum_{i=1}^{6}\left[V_{1i} + \frac{1}{2\gamma_{1i}}(\alpha_i - \alpha_i^*)^2 + \frac{1}{2\gamma_{2i}}(\beta_i - \beta_i^*)^2\right] \quad (21)$$

where $\alpha_i^*, \beta_i^*, \gamma_{1i}$ and γ_{2i} are some positive constants, and V_{1i} is given by:

$$V_{1i} = \boldsymbol{\zeta}_i^T \boldsymbol{P}_i \boldsymbol{\zeta}_i \quad (22)$$

where $\boldsymbol{\zeta}_i^T = \left[|\sigma_i|^{1/2}\text{sign}(\sigma_i), v_i\right]$ and $\boldsymbol{P}_i$ is given by:

$$\boldsymbol{P}_i = \boldsymbol{P}_i^T = \begin{bmatrix}\lambda_i + 4\varepsilon_i^2 & -2\varepsilon_i\\ -2\varepsilon_i & 1\end{bmatrix} > 0 \quad (23)$$

To ensure that derivative of V_{1i} is negative-definite, α_i must satisfy the following inequality:

$$\alpha_i > \frac{\varepsilon_i\delta_i + (\lambda_i + 4\varepsilon_i^2)(2\varepsilon_i + \delta_i) + \varepsilon_i}{\lambda_i} \quad (24)$$

and β_i must satisfy (17). Then, the time derivative of V_{2i} can be expressed as (see (29) and (30) in [19]):

$$\dot{V}_{2i} \le -\kappa_i\sqrt{V_{2i}} + \xi_i \quad (25)$$

where $\kappa_i = \min(\rho_i, \omega_{1i}, \omega_{2i})$ and $\rho_i = \frac{2\varepsilon_i\lambda_{\min}^{1/2}(\boldsymbol{P}_i)}{\lambda_{\max}(\boldsymbol{P}_i)}$, where $\lambda_{\min}(\boldsymbol{P}_i)$ and $\lambda_{\max}(\boldsymbol{P}_i)$ is minimum and maximum eigenvalue of matrix $\boldsymbol{P}_i$, respectively. Here, ξ_i is given by:

$$\xi_i = -|\alpha_i - \alpha_i^*|\left(\frac{1}{\gamma_{1i}}\dot{\alpha}_i - \frac{\omega_{1i}}{\sqrt{2\gamma_{1i}}}\right) - |\beta_i - \beta_i^*|\left(\frac{1}{\gamma_{2i}}\dot{\beta}_i - \frac{\omega_{2i}}{\sqrt{2\gamma_{2i}}}\right) \quad (26)$$

We must assure that $\xi_i = 0$, which is to be achieved through adaptation of the gains α_i and β_i, defined as follows:

$$\begin{aligned}\dot{\alpha}_i &= \omega_{1i}\sqrt{\frac{\gamma_{1i}}{2}}\\ \dot{\beta}_i &= \omega_{2i}\sqrt{\frac{\gamma_{2i}}{2}}\end{aligned} \quad (27)$$

Therefore, for the finite time convergence of $\boldsymbol{\sigma}$ and $\dot{\boldsymbol{\sigma}}$, α_i must satisfy inequality (24) via the adaptive equation in (27). By choosing

$$\varepsilon_i = \frac{\omega_{2i}\sqrt{\gamma_{2i}}}{2\omega_{1i}\sqrt{\gamma_{1i}}} \quad (28)$$

the ABSTSMC proposed in (17) is validated. Consequently, the tracking error converges asymptotically to zero.

IV. Simulation Results

In this section, the AUV model and controller are simulated in ROS2 using Gazebo, as shown in Fig. 2, to evaluate performance under a thruster fault condition. The 3D spiral curve is derived from the equations presented in [6], and is expressed as follows:

$$\begin{aligned}x_d(t) &= x_d(0) + U_d\big(1 - cos(\psi_d(t))\big)\\ y_d(t) &= y_d(0) + U_d sin(\psi_d(t))\\ z_d(t) &= z_d(0) + w_d t\\ \phi_d(t) &= 0\\ \theta_d(t) &= 0\\ \psi_d(t) &= \psi_d(0) + r_d t\end{aligned}$$

where $U_d = 4$, $w_d = -0.06$, $r_d = 0.2$, $x_d(0) = 0$, $z_d(0) = -0.2$, and $\psi_d(0) = 0$.

The desired trajectory $\boldsymbol{\eta}_d$ and the actual trajectories $\boldsymbol{\eta}$s under the BSTSMC and ABSTSMC are shown in Fig. 3, 4, and 5. The thrust forces for each method are shown in Fig. 6 and 7.

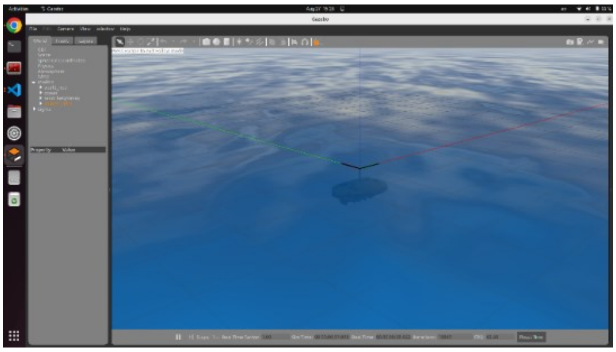

Fig. 2 AUV Gazebo simulation

The tracking performance of the BSTSMC and ABSTSMC is evaluated using two metrics: Maximum Absolute Error (MaxAE) and Mean Integral Absolute Error (MIAE):

$$\text{MaxAE} = \max_{t\in[T_1,T_2]} \left|\eta_i(t) - \eta_{d,i}(t)\right| \quad (29)$$

$$\text{MIAE} = \frac{1}{T_2 - T_1}\int_{T_1}^{T_2} \left|\eta_i(t) - \eta_{d,i}(t)\right| dt \quad (30)$$

where $[T_1, T_2]$ represents the interval for performance evaluation, $\eta_i(t)$ denotes the actual position and orientation of the AUV, $\eta_{d,i}(t)$ is the desired position and orientation of the AUV, with $i = 1, 2, 3, 4, 5, 6$.

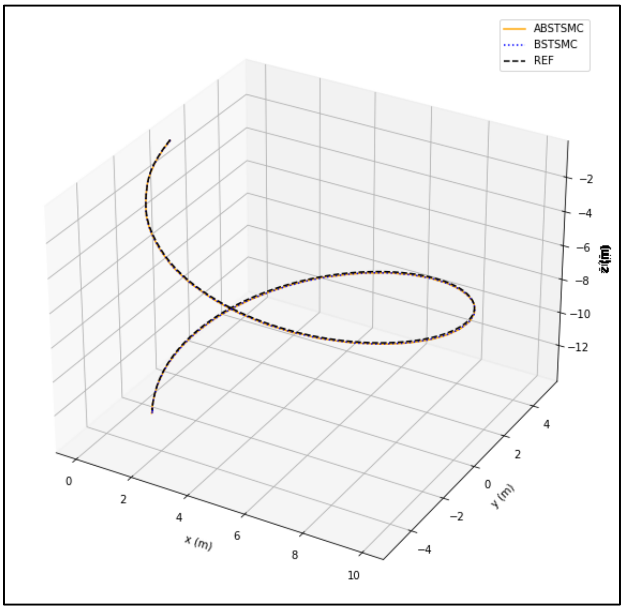

Fig. 3 AUV trajectories for the 3D spiral curve

The tracking error performance of the BSTSMC and ABSTSMC is evaluated over the time interval of 0 to 165 seconds using the same metrics, as shown in Tables I and II. The steady-state tracking error, evaluated during the period from 165 to 180 seconds after the AUV has settled, is presented in Tables III and IV.

The maximum absolute values and mean integral absolute values of thrust forces generated from eight thrusters are shown in Table V and VI. The parameters in STA with adaptive gains were set to $\boldsymbol{\varepsilon} = 0.01 \times \mathbf{I}_{6\times6}$, $\boldsymbol{\lambda} = 0.1 \times \mathbf{I}_{6\times6}$, $\boldsymbol{\gamma}_1 = 0.1 \times \mathbf{I}_{6\times6}$, and $\boldsymbol{\omega}_1 = 0.01 \times \mathbf{I}_{6\times6}$ where $\mathbf{I}_{6\times6}$ is the 6×6 identity matrix.

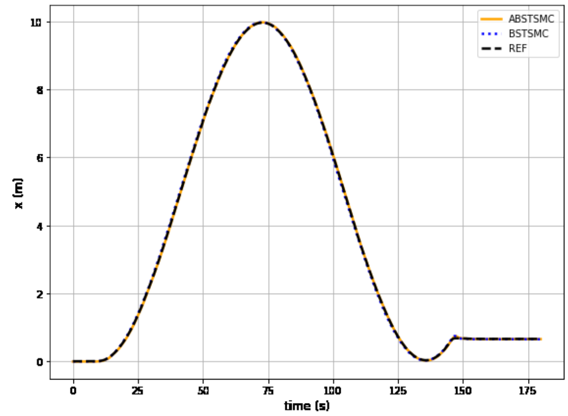

(a)

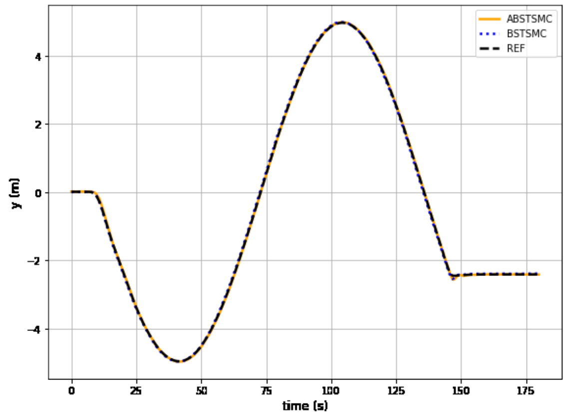

(b)

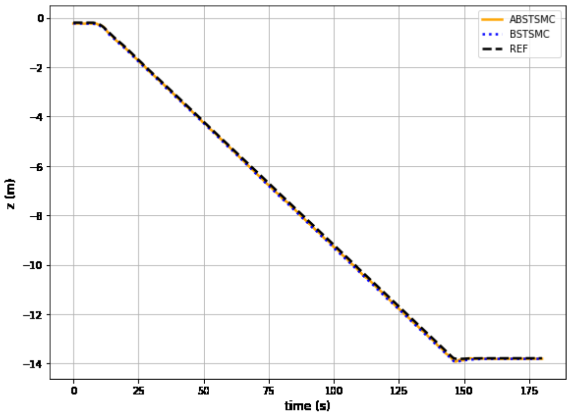

(c)

Fig. 4 AUV position for the 3D spiral curve: (a) Position along the x-axis, (b) Position along the y-axis, (c) Position along the z-axis.

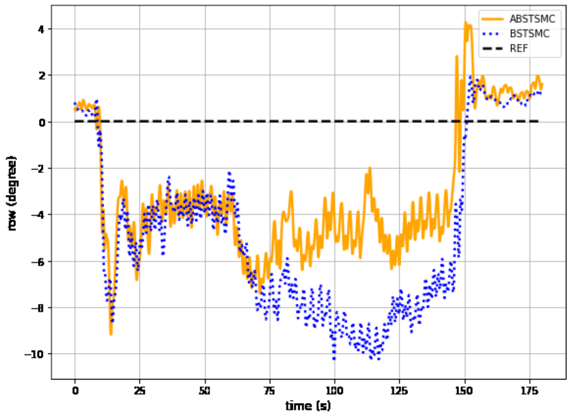

(a)

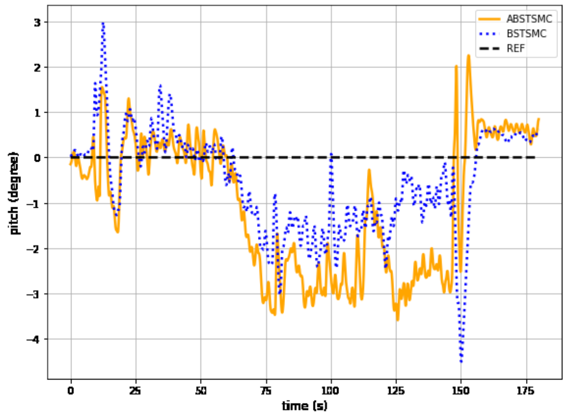

(b)

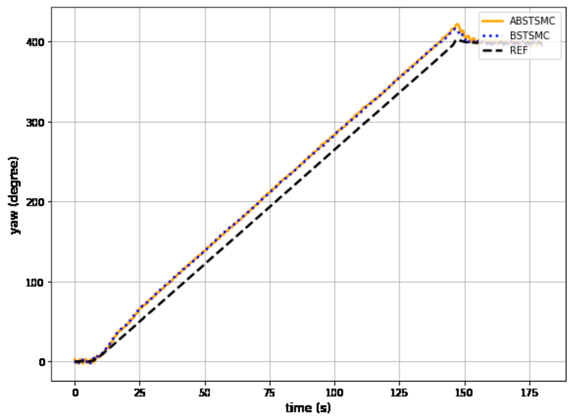

(c)

Fig. 5 AUV orientation for the 3D spiral curve: (a) Orientation about the x-axis, (b) Orientation about the y-axis, (c) Orientation about the z-axis.

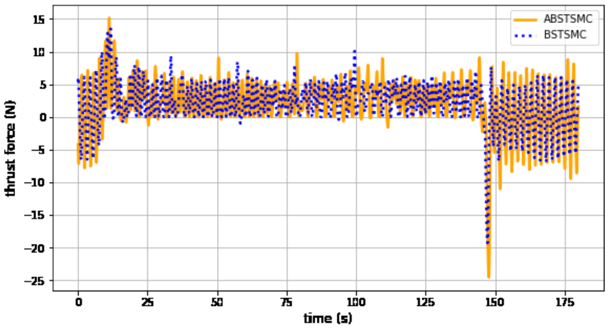

(a)

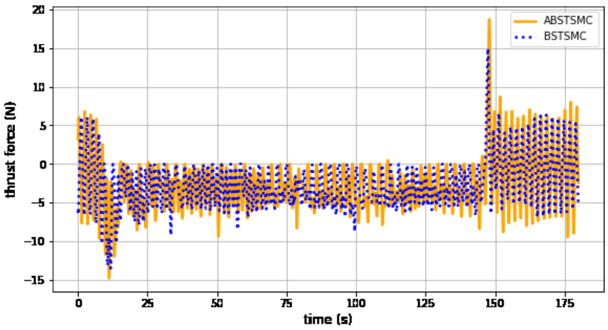

(b)

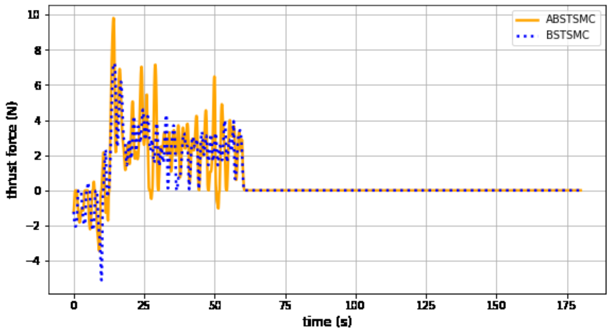

(c)

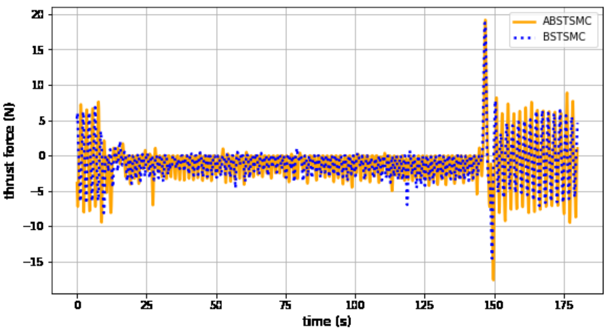

(d)

Fig. 6 Thrust forces generated by thrusters #1 to #4 for the 3D spiral curve: (a) Thruster #1, (b) Thruster #2, (c) Thruster #3, (d) Thruster #4.

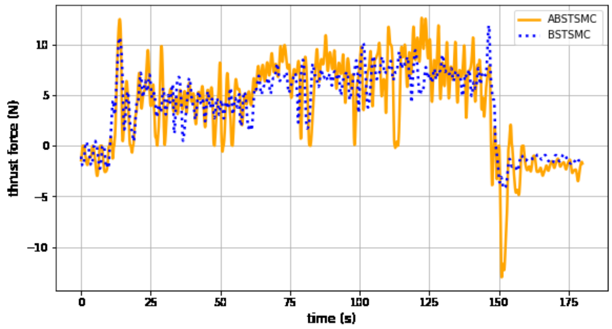

(a)

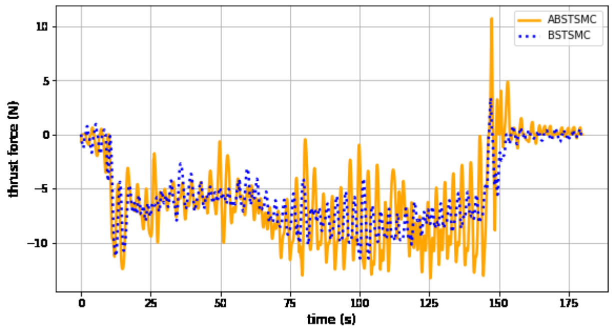

(b)

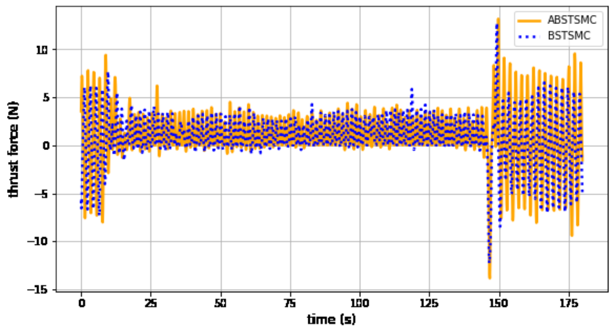

©

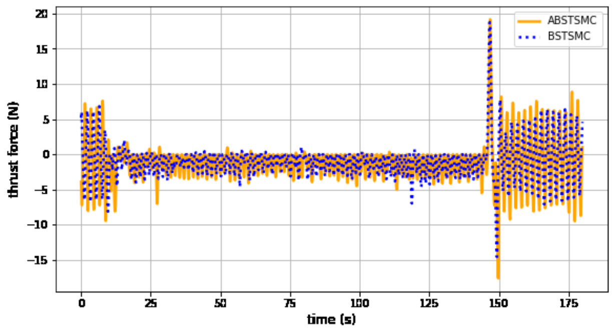

(d)

Fig. 7 Thrust forces generated by thrusters #5 to #8 for the 3D spiral Curve: (a) Thruster #5, (b) Thruster #6, (c) Thruster #7, (d) Thruster #8.

TABLE I
TRACKING ERRORS (MAXAE)

position and orientation	BSTSMC	ABSTSMC	% relative to BSTSMC
$x\ (m)$	0.0939	0.0593	-36.85
$y\ (m)$	0.1037	0.1170	12.83
$z\ (m)$	0.1465	0.1161	-20.75
$\phi\ (degree)$	10.3382	9.1756	-11.25
$\theta\ (degree)$	4.5049	3.5918	-20.27
$\psi\ (degree)$	19.8106	21.5047	8.55

TABLE II
TRACKING ERRORS (MIAE)

position and orientation	BSTSMC	ABSTSMC	% relative to BSTSMC
$x\ (m)$	0.0299	0.0119	-60.20
$y\ (m)$	0.0352	0.0146	-58.52
$z\ (m)$	0.0808	0.0564	-30.20
$\phi\ (degree)$	5.2471	3.7845	-27.87
$\theta\ (degree)$	0.9716	1.4350	47.69
$\psi\ (degree)$	13.3509	13.6151	1.98

TABLE III
STEADY-STATE TRACKING ERRORS (MAXAE)

position and orientation	BSTSMC	ABSTSMC	% relative to BSTSMC
$x\ (m)$	0.0113	0.0118	4.42
$y\ (m)$	0.0249	0.0053	-78.71
$z\ (m)$	0.0270	0.0279	3.33
$\phi\ (degree)$	1.3454	1.9676	46.25
$\theta\ (degree)$	0.6180	0.8425	36.33
$\psi\ (degree)$	3.2292	4.5170	39.88

TABLE IV
STEADY-STATE TRACKING ERRORS (MIAE)

position and orientation	BSTSMC	ABSTSMC	% relative to BSTSMC
$x\ (m)$	0.0082	0.0070	-14.63
$y\ (m)$	0.0211	0.0020	-90.52
$z\ (m)$	0.0247	0.0247	0.00
$\phi\ (degree)$	0.9641	1.3361	38.59
$\theta\ (degree)$	0.4564	0.6207	36.00
$\psi\ (degree)$	1.5016	1.7521	16.68

TABLE V
MAX ABSOLUTE VALUE OF THRUSTER FORCES (N)

Thruster No.	BSTSMC	ABSTSMC	% relative to BSTSMC
1	19.2739	24.5171	27.2
2	14.9668	18.7160	25.05
3 (Fault)	-	-	-
4	16.4010	14.3324	-12.61
5	11.8590	12.9679	9.35
6	11.4670	13.2923	15.92
7	12.7368	13.8536	8.77
8	18.7710	19.1895	2.23

TABLE VI
MEAN INTEGRAL ABSOLUTE VALUE OF THRUSTER FORCES (N)

Thruster No.	BSTSMC	ABSTSMC	% relative to BSTSMC
1	3.0246	3.2851	8.61
2	3.3834	3.5443	4.76
3 (Fault)	-	-	-
4	5.6551	5.1746	-8.5
5	4.8100	5.1457	6.98
6	5.5218	5.8199	5.4
7	1.7725	2.0066	13.21
8	1.8047	2.0819	15.36

Tables I and II show that ABSTSMC achieves better performance than BSTSMC in position tracking under unknown perturbations, based on the MaxAE and MIAE of tracking errors. Conversely, as indicated in Tables III and IV, BSTSMC performs more effectively in orientation tracking when considering the MaxAE and MIAE of steady-state errors. Additionally, Tables V and VI reveal that in the event of a failure in thruster #3, the overall forces of all thrusters, except for thruster #4, increase in the ABSTSMC due to gain adjustments.

V. CONCLUSION

This research presents comparative analysis of BSTSMC and ABSTSMC approaches for controlling AUV under thruster fault conditions in the presence of ocean currents. Simulation results show that both BSTSMC and ABSTSMC enable AUV to follow a reference trajectory accurately, even when faced with unexpected disturbances and thruster faults.

In future work, we plan to conduct pool tests of the Xplorer-mini AUV using both control algorithms to evaluate their performance under real-world conditions.

ACKNOWLEDGMENT

This work was supported by Rovula (Thailand) Co., Ltd., which included technical assistance in the form of specialized equipment and expert consultancy.

REFERENCES

[1] T. I. Fossen, *Guidance and Control of Ocean Vehicles*. Chichester, West Sussex, England: John Wiley & Sons, 1994.

[2] T. I. Fossen, *Handbook Of Marine Craft Hydrodynamics And Motion Control*, 2nd ed. Hobenken, NJ, USA: John Wiley & Sons, 2021.

[3] D. A. Smallwood and L. L. Whitcomb, "Model-based dynamic positioning of underwater robotic vehicles: theory and experiment," *IEEE Journal of Oceanic Engineering*, vol. 29, no. 1, pp. 169-186, Jan. 2004.

[4] T. Elmokadem, M. Zribi, and K. Youcef-Toumi, "Terminal sliding mode control for the trajectory tracking of underactuated Autonomous Underwater Vehicles," *Ocean Engineering*, vol. 129, pp. 613–625, 2017.

[5] C. Shen, B. Buckham, and Y. Shi, "Modified C/GMRES Algorithm for Fast Nonlinear Model Predictive Tracking Control of AUVs," *IEEE Transactions on Control Systems Technology*, vol. 25, no. 5, pp. 1896–1904, Sep. 2017.

[6] W. Yujia, Z. Mingjun, A. W. Philip, and L. Xing, "Adaptive neural network-based backstepping fault tolerant control for underwater vehicles with thruster fault," *Ocean Engineering*, vol. 110, pp. 15-24, 2015.

[7] O. Elhaki and K. Shojaei, "Neural network-based target tracking control of underactuated autonomous underwater vehicles with a prescribed performance," *Ocean Engineering*, vol. 167, pp. 239–256, Nov. 2018..

[8] C. Hou, X. Li, H. Wang, P. Zhai, and H. Lu, "Fuzzy linear extended states observer-based iteration learning fault-tolerant control for autonomous underwater vehicle trajectory-tracking system," *IET Control Theory & Applications*, vol. 17, no. 3, pp. 270–283, 2022.

[9] W. Xu, Y. Xiao, H. Li, J. Zhang, and H. Zhang, "Trajectory Tracking for Autonomous Underwater Vehicle Based on Model-Free Predictive Control," in *Proc. 2019 IEEE 20th International Conference on High Performance Switching and Routing (HPSR)*, Xi'an, China, 2019, 2019, pp. 1–6.

[10] Q. Zhang, J. Lin, Q. Sha, B. He, and G. Li, "Deep Interactive Reinforcement Learning for Path Following of Autonomous Underwater Vehicle," *IEEE Access*, vol. 8, pp. 24258–24268, 2020.

[11] J. Guerrero, J. Torres, V. Creuze, and A. Chemori, "Trajectory tracking for autonomous underwater vehicle: An adaptive approach," *Ocean Engineering*, vol. 172, pp. 511–522, 2019.

[12] Y. Shtessel, M. Taleb, and F. Plestan, "A novel adaptive-gain super twisting sliding mode controller: Methodology and application," *Automatica*, vol. 48, no. 5, pp. 759–769, 2012.

[13] Y. Zheping, W. Man, and X. Jian, “Robust adaptive sliding mode control of underactuated autonomous underwater vehicles with uncertain dynamics,” *Ocean Engineering*, vol. 173, pp. 802–809, 2019.

[14] D. Ao, W. Huang, P. K. Wong, and J. Li, “Robust Backstepping Super-Twisting Sliding Mode Control for Autonomous Vehicle Path following,” *IEEE Access*, vol. 9, pp. 123165–123177, 2021.

[15] G. Peng, Y. Zheping, Z. Wei, and T. Jialing, "Trajectory tracking control for autonomous underwater vehicles based on dual closed-loop of MPC with uncertain dynamics," *Ocean Engineering*, vol. 265, 2022.

[16] D. Peizhou, Y. Wencheng, W. Yingqiang, H. Ruoyu, C. Ying, and S. H. Huang, "A novel adaptive backstepping sliding mode control for a lightweight autonomous underwater vehicle with input saturation," *Ocean Engineering*, vol. 263, 2022.

[17] G. Xia, Y. Zhang, W. Zhang, K. Zhang, and H. Yang, “Robust adaptive super-twisting sliding mode formation controller for homing of multi-underactuated AUV recovery system with uncertainties,” *ISA transactions*, vol. 130, pp. 136–151, 2022.

[18] B. Li, X. Gao, H. Huang, and H. Yang, “Improved adaptive twisting sliding mode control for trajectory tracking of an AUV subject to uncertainties,” *Ocean Engineering*, vol. 297, 2024.

[19] B. S. Yuri, A. M. Jaime, P. Franck, M. F. Leonid, and S. P. Alexander, "Super-twisting adaptive sliding mode control: A Lyapunov design," *in Proc. 49th IEEE Conference on Decision and Control (CDC),* Atlanta, GA, USA, 2010*,* pp. 5109-5113.

[20] A. Levant, "Sliding order and sliding accuracy in sliding mode control," *International Journal of Control*, vol. 58, no. 6, pp. 1247-1263, 1993.

[21] Y. Shtessel, C. Edwards, L. Fridman, Arie Levant, *Sliding Mode Control and Observation*. New York, NY, USA: Birkhauser, 2014.

[22] V. Utkin, A. Poznyak, Y. Orlov, A. Polyakov, "Conventional and high order sliding mode control," *Journal of the Franklin Institute*, vol 357, no. 15, pp. 10244-10261, 2020.

Warit Tanaprasitpattana received his B.Eng. degree (with honors) in Electrical Engineering from Kasetsart University, Bangkok, Thailand, in 2023.

He is currently a research assistant and is pursuing an M.Eng. in Electrical Engineering at Kasetsart University, Bangkok, Thailand. His primary research interests include control theory, artificial intelligence and data-driven control, with applications in vibration systems and underwater robotics.

Peerayot Sanposh received his B.Eng. degree (with honors) in Electrical Engineering from Kasetsart University, Bangkok, Thailand, in 1995. He earned his M.S. degree in Electrical Engineering: Systems from the University of Michigan, Ann Arbor, MI, USA, in 1997, and both his M.S. and Ph.D. degrees in Systems Science and Mathematics from Washington University, Saint Louis, MO, USA, in 1999 and 2001, respectively.

In 1995, he joined the Department of Electrical Engineering at Kasetsart University, Bangkok, Thailand, where he is currently an Associate Professor. His research interests include optimal control, process control, robust control, and robotics. His recent work focuses on autonomous underwater vehicles, autonomous sailboats, agricultural robots, energy-efficient control, and vibration control.

Benjaset Maneeloke received his B.Eng. degree (with honors) in Electrical Engineering from Kasetsart University, Bangkok, Thailand, in 2023.

He is currently a research assistant and is pursuing an M.Eng. in Electrical Engineering at Kasetsart University, Bangkok, Thailand. His primary research interests include control theory, artificial intelligence and data-driven control, with applications in vibration systems and underwater robotics.

Nattakit Techajaroonjit received his B.Eng. degree in Electrical-Mechanical Manufacturing Engineering from Kasetsart University, Bangkok, Thailand, in 2020.

He is currently a research assistant and is pursuing an M.Eng. in Computer Engineering at Kasetsart University, Bangkok, Thailand. His primary research interests include automation, software development, control theory, artificial intelligence, data-driven control, with applications in biped humanoid robot, autonomous sailboats and marine robots.

Vasutorn Siriyakorn received his B.Eng**.** degree **(**with honors**)** in computer engineering from Kasetsart University, Bangkok, Thailand, in 2018**.**

During his studies, he actively participated in and received awards from several autonomous robot competitions, such as RoboSub, RoboCup, and SAUVC**.** He also participated in the Thai-German S&T Cooperation project, conducting joint research on structural control and health monitoring for smart city Infrastructures at Fraunhofer-LBF Institute**.** He is interested in advanced control systems, underwater vehicle control, fault tolerance control for mobile robots, and embedded control systems**.**

He is currently a research assistant at Faculty of Engineering, Kasetsart University, Bangkok, Thailand**.** His research focuses on software development, embedded systems, internet of things and realcontrol systems for autonomous underwater vehicles and ground source heat pump systems**.**

Yodyium Tipsuwan received B.Eng**.** degree **(**with honors**)** in computer engineering from Kasetsart University, Bangkok, Thailand, in 1996, and his M.S. and Ph.D. degrees in electrical engineering from North Carolina State University, Raleigh, USA, in 1999 and 2003, respectively**.** He obtained a Certificate in Quantitative Finance from the CQF Institute in 2019**.**

He is currently an Assistant Professor in the Department of Computer Engineering at Kasetsart University**.** His main research interests include computational finance, machine learning, embedded systems, control systems, and robotics**.**

Weerawut Charubhun received his B.S**.** in Mechanical Engineering from Kasetsart University, Bangkok, Thailand, in 1998, and his M**.**S**.** in Mechanical Engineering from the University of Sydney, Sydney, Australia, in 2022**.**

Since May 2021, he has been leading the robotics team at ROVULA **(**Thailand**)** as Robotics Team Lead**.** He manages a cross-functional team of mechanical, electrical, and software engineers in the design and development of autonomous underwater vehicles **(**AUVs**)** and unmanned surface vehicles **(**USVs**).** Additionally, he collaborates with Kasetsart University on a research project to integrate advanced control algorithms and path planning techniques into AUVs**.**